Acta Mech 228, 673–681 (2017)
DOI 10.1007/s00707-016-1730-2

ORIGINAL PAPER

Xianzhong Xie · Xia Hu · Jian Peng · Zhiqian Wang

Refined modeling and free vibration of two-span suspended transmission lines

Received: 6 January 2016 / Revised: 4 May 2016 / Published online: 7 October 2016

Abstract The dynamic behavior of two-span suspended transmission lines is studied. The equations of the two-span transmission lines are obtained with the help of Hamilton's principle. Meanwhile, the boundary and continuity conditions are ensured by the mechanics equilibrium condition. Then setting the determinant of the coefficient matrix equal to zero, the exact eigenvalues can be given. Then, the results of the parametric analysis of the in-plane and out-of-plane eigenproblems are presented, and the frequency avoidance phenomena are introduced. Finally, the possible nonlinear interaction of two-span transmission lines is examined.

1 Introduction

The transmission line is a part of large span suspension cable structures. It is a flexible and light structure, widely used in several engineering applications [1]. Due to their natural aptitude to perform large displacements, in recent decades, they have been the focus of many researches conducted on nonlinear dynamics. Statics and linear free dynamics of suspended horizontal and inclined cables were studied [2]. Afterward, pioneering papers addressed nonlinear free dynamics, with special interest on frequency–amplitude relations and internal resonances [3].

As far as the transmission lines or cables are concerned, a great deal of research has appeared on the matter of nonlinear free and forced oscillations, regarding both the theoretical formulation of the problem and the analysis of the structural behavior [2–9]. Moreover, the nonlinear response of elastic cables with the flexural stiffness or flexural-torsional stiffness is considered [10,11]. Obviously, these studies are important for understanding the large amplitude vibration mechanism of the cables. However, only the single cable was considered. Therefore, the dynamic interaction between the different span cables cannot be reflected. In fact, this kind of interaction has been verified by numerical investigation, analytical and experimental investigation [12–17]. The transmission line can be simulated by several lumped masses connected by elastic elements [18]. After establishing the kinetic energy and potential energy of the transmission line, the mass and stiffness matrices can be determined through partial differential calculation [19].

Generally speaking, the two-span suspended transmission line system exhibits a coupling characteristic, which is mainly governed by the force continuity conditions. Therefore, the accurate mathematical description for the force continuity conditions of the system plays an important role in modeling of the two-span suspended

X. Xie (✉) · X. Hu · J. Peng
School of Civil Engineering, Hunan University of Science and Technology, Xiangtan 411201, Hunan, People's Republic of China
E-mail: xianzhongx@163.com
Tel.: +86-731-58290251

Z. Wang
College of Civil Engineering and Mechanics, Central South University of Forestry and Technology, Changsha 410004, Hunan, People's Republic of China

transmission line system. The objective of the present paper is to develop a general dynamic model for the two-span suspended transmission lines. First, we should keep the distinction between the two kinds of conditions. So the paper also aims to demonstrate the boundary and connection conditions. Because of the particularity of the connection condition, the analysis should consider both statics and dynamics. A set of nonlinear partial differential equations governing the motion of the power transmission line is derived using the boundary and connection conditions. Afterward, the homogeneous linearized equations are solved with eigenvalues. In particular, a nonlinear model representative of planar vibrations is to be introduced in detail in the follow-up work.

In this study, the main objective is to derive the refined model of two-span suspended transmission lines. Some attention is focused on the natural frequencies and mode shapes of the two-span transmission lines. The paper is organized as follows. In Sect. 2, the nonlinear motion equations of two-span transmission lines are derived using Hamilton's principle. Section 3 performs the eigenvalue analysis of the in-plane and out-of-plane linear problem. Moreover, the possible internal resonances in the two-span transmission lines are summarized. The effects of the angle at the central support is discussed in Sect. 4. A short summary of results and remarks is presented in Sect. 5.

2 The mathematical model

In this study, we first dynamically formulate the modeling of the two-span transmission lines. Two Cartesian Coordinate systems are chosen to derive the equations of motion, as shown in Fig. 1. For the coordinate system $O_1 - x_1 y_1 z_1$ ($O_2 - x_2 y_2 z_2$), the origin $O_{(1,2)}$ is placed at one of the supports of the cables. The static (dashed line) and dynamic (solid line) configurations of the power transmission line are shown in Fig. 1. The three-dimensional displacements of the cables are denoted by $U_1(x_1, t)$ ($U_2(x_2, t)$), $V_1(x_1, t)$ ($V_2(x_2, t)$) and $W_1(x_1, t)$ ($W_2(x_2, t)$) along the $x_1(x_2)$, $y_1(y_2)$ and $z_1(z_2)$ directions, respectively. Moreover, we assume that the bending and torsional shear rigidities of the cable are neglected. In addition, m is the mass per unit length of the cables; $l_{1,2}$ is the span of the cable; E_c is the Young's modulus of the cable; A_c is the cross-section area of the cable; C_u, C_v and C_w are the viscous damping coefficients of the cable per unit length; g is the gravitational acceleration. At the central support, the kind of restraint is hinge, and θ_1, θ_2 are the angles between the dynamic internal tension T_i and the y axis (see Fig. 1b).

The motion equations and corresponding boundary conditions of power transmission line can be obtained by using the extended Hamilton's principle, which may be expressed as

$$\int_{t_1}^{t_2} \delta(T - U)\mathrm{d}t + \int_{t_1}^{t_2} \delta W \mathrm{d}t = 0, \tag{1}$$

where T is the kinetic energy, U is the strain energy of the transmission line, δW is the sum of the variation of the potential energy and the virtual work of non-conservative forces, and δ is the first variation.

To facilitate the parametric study, the following nomenclature is used: The planar static of the cable catenary curve is attained along the cable chord, with x_i being the space variable:

$$y_i(x_i) = 4d_i \left[\frac{x_i}{l_i} - \left(\frac{x_i}{l_i} \right)^2 \right], \quad i = 1, 2, \tag{2}$$

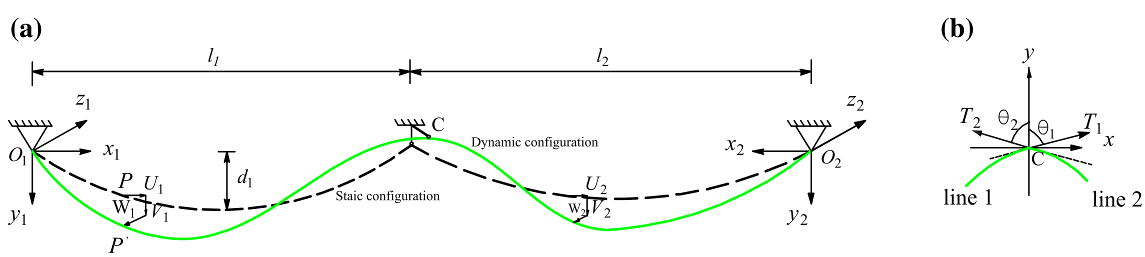

Fig. 1 The configurations of the model, **a** the two-span transmission lines; **b** the configurations of the central support

where d_i is the sag of the cable, and H_i is the horizontal component of the cable tension specified by

$$H_i = \frac{mgl_i^2}{8d_i}, \quad i = 1, 2. \tag{3}$$

Of course, under the previous assumptions and by using the classical Hamilton's principle, the equations of in-plane and out-of-plane motion can be obtained:

$$m\ddot{U}_i + C_u\dot{U}_i = \frac{\partial}{\partial x}\left[\left(H_i + E_cA_c\varepsilon\left(x_i, t\right)\right)\left(U_i{}'\right)\right], \tag{4}$$

$$m\ddot{V}_i + C_v\dot{V}_i - mg = \frac{\partial}{\partial x}\left[\left(H_i + E_cA_c\varepsilon\left(x_i, t\right)\right)\left(y_i' + V_i{}'\right)\right], \tag{5}$$

$$m\ddot{W}_i + C_w\dot{W}_i = \frac{\partial}{\partial x}\left[\left(H_i + E_cA_c\varepsilon\left(x_i, t\right)\right)\left(W_i{}'\right)\right]. \tag{6}$$

Considering the static configuration, we can assume a quasi-static stretching during the cable motion. Following this assumption, neglecting the acceleration and velocity terms in Eq. (4), and considering the boundary condition of the cable, the displacement $U_i(x_i, t)$ can be expressed as:

$$U_i(x_i, t) = \frac{x_i}{l_i}\int_0^{l_i}\left(y_{i,x_i}V_{i,x_i} + \frac{V_{i,x_i}^2 + W_{i,x_i}^2}{2}\right)\mathrm{d}x_i - \int_0^{x_i}\left(y_{i,x_i}V_{i,x_i} + \frac{V_{i,x_i}^2 + W_{i,x_i}^2}{2}\right)\mathrm{d}x_i. \tag{7}$$

In this case, the approximate dynamic strain of the cable can be written as:

$$\varepsilon(x_i, t) = \frac{1}{l_i}\int_0^{l_i}\left(y_{i,x_i}V_{i,x_i} + \frac{V_{i,x_i}^2 + W_{i,x_i}^2}{2}\right)\mathrm{d}x_i. \tag{8}$$

Under the previous assumptions, in what follows, to ensure the continuity of the two-span transmission line, the following conditions at the connection point of the cables ($x_1 = l_1, x_2 = l_2$) should hold:
Force conditions:

$$T_1 \sin\theta_1 = T_2 \sin\theta_2. \tag{9}$$

Thus, the dynamic internal tension T_i is related to the strain as $T_i = E_cA_c\varepsilon(x_i, t)$. In here, because of the swing angle of the transmission line insulators is very small, so the tension of the transmission line insulators are neglected in the force conditions.
Displacement conditions:

$$\begin{aligned}
&U_1(l_1)\cos\left(\frac{\pi}{2} - \theta_1\right) - V_1(l_1)\sin\left(\frac{\pi}{2} - \theta_1 - \theta_2\right) = U_2(l_2),\\
&U_1(l_1)\sin\left(\frac{\pi}{2} - \theta_1\right) + V_1(l_1)\cos\left(\frac{\pi}{2} - \theta_1 - \theta_2\right) = V_2(l_2),\\
&W_1(l_1) = W_2(l_2).
\end{aligned} \tag{10}$$

From the above analysis, the boundary and continuity conditions can be established by using the boundary conditions, continuity conditions of the displacements and equilibrium conditions of the force. Specifically, the force conditions (Eq. 9) include the effects of the angle at the central support and the contribution of the static configuration. It should be pointed out that the force conditions also reflect the contribution of the static and dynamic configuration to the angle at the central support.

In order to write non-dimensional equations, the following normalization is introduced:

$$\begin{aligned}
&x^*{}_i = \frac{x_i}{l_i};\, v_i = \frac{V_i}{l_i};\, w_i = \frac{W_i}{l_i};\, y^*{}_i = \frac{y_i}{d_i};\, b_i = \frac{d_i}{l_i};\, u_i = \frac{U_i}{l_i};\, C_v^* = \frac{C_V}{m\omega_1};\\
&C^*{}_w = \frac{C_W}{m\omega_1};\, \tau = \omega_1 t;\, \alpha = \frac{E_cA_c}{H};\quad i = 1, 2,
\end{aligned} \tag{11}$$

where ω_1 is the first natural frequency of the in-plane motion. Respectively, the overdot and prime indicate the derivatives with respect to t and x. The non-dimensional frequency parameters are defined as:

$$\varepsilon^*(t) = \int_0^1 [by^{*\prime}v' + \frac{1}{2}(v')^2 + \frac{1}{2}(w')^2]\mathrm{d}x. \tag{12}$$

Therefore, the non-dimensional equations of motion become

$$\ddot{v}_i - \frac{1}{{\omega_v}^2}\left[{v_i}' + \alpha(by' + {v_i}')\varepsilon(t)\right]' = 0, \tag{13}$$

$$\ddot{w}_i - \frac{1}{{\omega_w}^2}\left[{w_i}' + \alpha {w_i}'\varepsilon(t)\right]' = 0, \tag{14}$$

where the asterisks are dropped for simplicity.

From the following sections, the eigenvalue problem of the non-dimensional motion equations is depicted. The modal analysis is performed considering the equations of motion linearized about the static equilibrium configuration, which means that the linear term will be considered. Therefore, it is assumed that the structural damping can be neglected. So the two sets of equations of in-plane motion and out-of-plane motion can be analyzed separately.

It is known that nonlinear systems exhibit extremely complex behavior which linear systems can not. These phenomena include jumps, bifurcations, saturation, subharmonic, superharmonic and internal resonances, resonance captures, limit cycles, modal interactions and chaos. But in this paper, the main focus is on the characterize of the linear modes. So in the companion manuscript, free nonlinear vibrations of the two-span transmission lines away from internal resonances are studied.

3 Eigenvalue analysis in the linear problem

If we neglect all nonlinear terms and damping, the system equations governing the linear undamped free vibration of the two-span suspended transmission line can be written as:

In-plane motion:

$$\ddot{v}_i - \frac{1}{{\omega_v}^2}\left[{v_i}' + \alpha\left(by' + {v_i}'\right)\int_0^1 by'v'\mathrm{d}x\right]' = 0. \tag{15}$$

Out-of-plane motion:

$$\ddot{w}_i - \frac{1}{{\omega_w}^2}\left[{w_i}' + \alpha {w_i}'\int_0^1 by'v'\mathrm{d}x\right]' = 0. \tag{16}$$

Next, we apply the separation-of-variables method to determine the natural frequencies and natural modes of the two-span suspended transmission lines.

3.1 In-plane eigenvalue problem

For this case, the general solution of the in-plane motion equation can be considered in the form

$$\mathbf{v} = \begin{bmatrix} v_1 \\ v_2 \end{bmatrix} = \begin{bmatrix} \phi_1(x) \\ \phi_2(x) \end{bmatrix} \mathrm{e}^{\mathrm{i}\frac{\omega_v}{\omega_1}\tau},\ x \in [0, 1], \tag{17}$$

where ω_v represents the in-plane natural frequency of the system. The use of separation of variables implies that the motion is synchronous; that is, different points, say the points at $x = x_1$ and x_2, obtain their maxima and minima at the same time although they may have different amplitudes $V(x)$. In other words, that means each of these mode shapes is related to a specific physical configuration of the system, which is a function of spatial coordinates within the structure, but not a function of time.

Taking Eq. (17) into Eqs. (13) and (14), it is assumed that the higher order term is going to be negative. Also the nonlinear term of the strain expansion equation is negative. In order to simplify the calculation, the differential equations that define the undamped normal mode shapes in both cables domains are:

$$\phi_1''(x) + {\omega_{v1}}^2\phi_1(x) = 8\alpha b\varepsilon_1, \tag{18}$$

$$\phi_2''(x) + {\omega_{v2}}^2\phi_2(x) = 8\alpha b_2\varepsilon_2, \tag{19}$$

with the following boundary and connection conditions:

$$\phi_1(1)\cos\theta_2 = \phi_2(1)\sin\theta_1, \tag{20}$$
$$E_c A_c \varepsilon_1 \sin\theta_1 = E_c A_c \varepsilon_2 \sin\theta_2, \tag{21}$$
$$\phi_1(0) = 0; \quad \phi_2(0) = 0, \tag{22}$$

where

$$\omega_{v2} = \omega_{v1}\frac{l_2}{l_1}. \tag{23}$$

The eigenvalue problem yields an infinite number of eigenvalues ω_v, linear undamped natural frequencies, corresponding to an infinite number of eigenfunctions $V(x)$, mode shapes. The non-dimensional modal stretching is given by

$$\varepsilon_i = \int_0^1 by'\phi_i{}'\mathrm{d}x_i. \tag{24}$$

It is found that the modal function in the cable domain is:

$$\phi_i(x) = d_{1i}\cos\omega_v x + d_{2i}\sin\omega_v x + \frac{8\alpha b}{{\omega_v}^2}\Gamma_i. \tag{25}$$

To solve Eq. (25), we let

$$\Gamma_i = \int_0^1 4b(1-2x_i)\phi_i{}'(x_i)\mathrm{d}x_i, \tag{26}$$

where, for a given ϕ_i, Γ_i is a constant, $i = 1, 2, \ldots$. Then, substituting Eq. (26) into Eq. (25) yields

$$4bd_{1i}(2\sin\omega_v - \omega_v\cos\omega_v - \omega_v) + 4bd_{2i}(2 - 2\cos\omega_v - \omega_v\sin\omega_v) - \omega_v\Gamma_i = 0. \tag{27}$$

Then, the determinant which determined to frequency of free vibrations of two-span transmission lines are as following:

$$\begin{vmatrix} 1 & 0 & \frac{8\alpha b}{\omega_v^2} & 0 & 0 & 0 \\ \cos\omega_v & \sin\omega_v & \frac{8\alpha b}{\omega_v^2} & \cos\theta_1\cos\omega_v & \cos\theta_1\sin\omega_v & \cos\theta_1\frac{8\alpha b}{\omega_v^2} \\ \nu & \varrho & -\omega_v & 0 & 0 & 0 \\ 0 & 0 & 0 & 1 & 0 & \frac{8\alpha b}{\omega_v^2} \\ 0 & 0 & 1 & 0 & 0 & 1 \\ 0 & 0 & 0 & \nu & \varrho & -\omega_v \end{vmatrix} = 0, \tag{28}$$

where $\nu = 4b(2\sin\omega_v - \omega_v\cos\omega_v - \omega_v)$, $\varrho = 4b(2 - 2\cos\omega_v - \omega_v\sin\omega_v)$.

Apply Eq. (28), we can obtain the natural frequency of the i-th mode ω_v. Then the corresponding i-th modal shape can be written as:

$$\phi_{1i}(x) = c\left[\cos\omega_{vi}x + \frac{1}{4b}\left(-4b\,(2\sin\omega_{vi} - \omega_{vi}\cos\omega_{vi} - \omega_{vi}) + \frac{{\omega_{vi}}^3}{8\alpha b}\right)\sin\omega_{vi}x - \frac{{\omega_{vi}}^2}{8\alpha b}\right], \tag{29}$$

$$\phi_{2i}(x) = c\frac{{\omega_{v1}}^2}{{\omega_{v2}}^2}\frac{\cos\theta_1}{\cos\theta_2}\left[\cos\omega_{vi}x + \frac{1}{4b}\left(-4b\,(2\sin\omega_{vi} - \omega_{vi}\cos\omega_{vi} - \omega_{vi}) + \frac{{\omega_{vi}}^3}{8\alpha b}\right)\sin\omega_{vi}x - \frac{{\omega_{vi}}^2}{8\alpha b}\right], \tag{30}$$

where the coefficient c can be determined with the normalization condition.

Next, applying the characteristic frequency equation, we will investigate the effects of the span ratio l_1/l_2 and the angles at the central support $\theta_{1,2}$ on the nondimensional natural frequencies with some numerical examples. We choose the dimensional parameters and material properties of the cable as follows: $l_1 = 120\,\mathrm{m}$, $E = 1.95 \times 10^5\,\mathrm{MPa}$, $A = 6.27 \times 10^{-3}\,\mathrm{m}^2$, $\theta_1 = \theta_2 = \pi/12$, $b = 0.005$. Figure 2 shows the variation of the in-plane natural frequencies of the two-span transmission lines with different parameters l_1/l_2. In particular, the horizontal straight lines represent the eigenvalues of the cable $(2\pi, 4\pi)$.

It is seen that frequency avoidance phenomena are illustrated by loci of the frequencies ω_v plotted versus l_1/l_2 for the transmission lines. As l_1/l_2 increases slowly, two curves of ω progressively approach each other at $l_1/l_2 \cong 1.5, 5.5$, and afterward abruptly diverge from each other. The sudden divergence avoids their crossing,

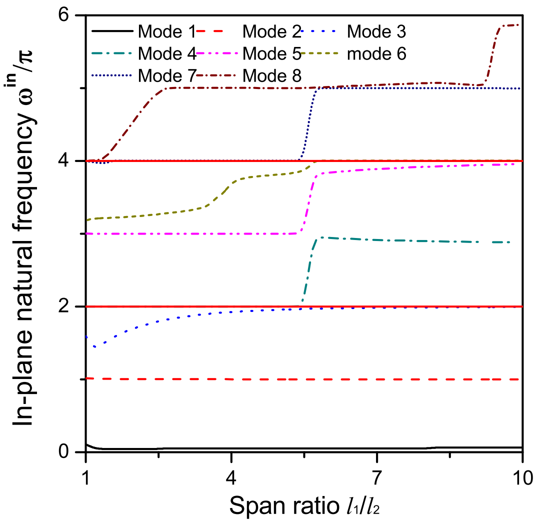

Fig. 2 Variation of the in-plane natural frequencies of the cable with the span ratio l_1/l_2

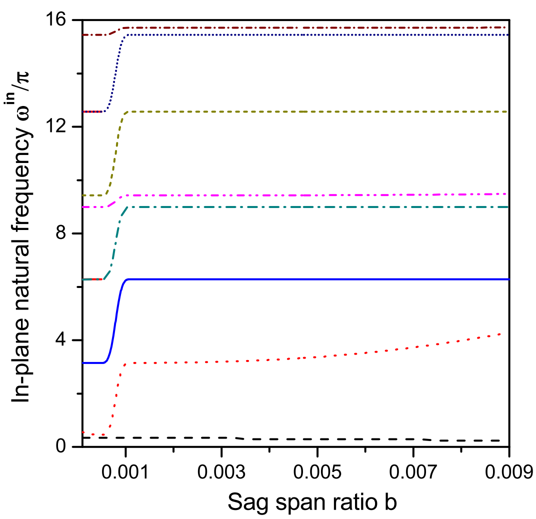

Fig. 3 In-plane system eigenvalue b-dependence

leading to an evident frequency veering phenomenon. Of course, this happens in a rapid but continuous way. At this crossover point, a multiple of the 1:1 internal resonance may be activated. It is demonstrated that both from theoretical and practical viewpoints, frequency avoidance phenomena, together with the coexisting hybrid modes, are actually related to planar dynamics, distinguishing inclined cables from horizontal cables that exhibit frequency crossover phenomena of symmetric/antisymmetric modes. It is seen that the values (ω_3, ω_4) approach each other and thereafter abruptly diverge from each other. In other words, to describe the sensitivity of the system, the nearness to avoided-crossing frequencies is achieved by varying the nonzero detuning parameter of the 1:1 resonance. Of course, other internal resonances occur in other forms: for example, investigating the frequencies of the system from ω_1 to ω_6 when a set of parameters have been fixed. Having a close-up view of the frequencies, other forms of the internal resonances such as (1:2, 1:3) occur.

In order to describe the modal properties better, the sag-to-span ratio b is used to investigate the effects. It is seen that the curve of the first eigenvalues of ω_v is a straight line almost in whole range of the sag-to-span b. From Fig. 3, $\theta_1 = \theta_2 = \pi/12$, $l_1/l_2 = 1$, it is noticed that when the eigenvalue comes to the third, the locus is mainly a straight line. That is to say the sag-to-span b could not affect the value of ω_v. But in a small range of b, close to 10^{-3}, the alteration appears. Obviously, the sag-to-span has a powerful effect on the value of the system frequency in a small range. The higher eigenvalue curves (fifth and eighth) are quite different. For example, the fifth locus increases slowly from $b = 10^{-4}$ to 10^{-3} and then keeps a straight line in a major

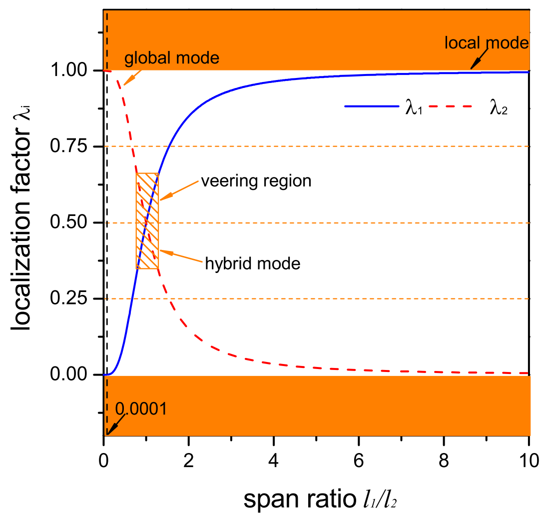

Fig. 4 Variation of the localization factor with the span ratio l_1/l_2

range, although the effect of the cable sag is small in this range. But corresponding to the second locus, it has some slightly different conventions. It shows a behavior for $b > 5 \times 10^{-3}$ which looks like an inverted parabol.

As is stated in Ref. [20], some mechanical properties of the transmission line are dissimilar. Therefore, the transmission line is prone to exhibit a mode localization phenomenon, and the vibration amplitude of one sub-system may be much larger than the one of the other sub-system [21]. Due to significant mass difference between two sub-systems, the large vibration amplitude of one sub-system cannot fully distinguish the strong mode localization phenomenon. Therefore, to more clearly illustrate this phenomenon and reflect the contribution of the sub-system eigenvalues to the mode shapes, the localization factor λ_i for the i-th mode is introduced, defined as [20]

$$\lambda_i = \frac{\int_0^1 m_{1,2}\phi|\varphi_i^2(x_{1,2})\mathrm{d}x_{1,2}}{\int_0^1 m_2\phi|\varphi_i^2(x_2)\mathrm{d}x_2 + \int_0^1 m_1\phi|\varphi_i^2(x_1)\mathrm{d}x_1}. \tag{31}$$

Obviously, the physical meaning of this factor is the mode kinematic energy ratio between the sub-system and the system. Figure 4 shows the variation of the localization factor of the lower order mode with the span ratio l_1/l_2. It is seen from Fig. 4 that the in-plane mode shape may exhibit the localization phenomenon ($\lambda_i > 0.65$) as the span ratio l_1/l_2 varies. Therefore, the mode shape exhibits a strong local characteristic, whereas the mode shape may exhibit a hybrid characteristic ($\lambda_i \approx 0.50$) when the *curve veering phenomenon* occurs or the parameter is close to the *crossover* region, as shown in Fig. 4.

3.2 Out-of-plane eigenvalue problem

The separation-of-variables method is introduced in this paper:

$$\mathbf{w} = \begin{bmatrix} w_1 \\ w_2 \end{bmatrix} = \begin{bmatrix} \psi_1(x) \\ \psi_2(x) \end{bmatrix} \mathrm{e}^{\mathrm{i}\frac{\omega}{\omega_1}\tau}, \quad x \in [0, 1]. \tag{32}$$

Similarly, the eigenmodes equations follow as

$$\psi_1{}''(x) + \omega_{w1}{}^2\psi_1(x) = 0, \tag{33}$$
$$\psi_2{}''(x) + \omega_{w2}{}^2\psi_2(x) = 0, \tag{34}$$

with the following boundary and connection conditions:

$$\psi_1(1) = \psi_2(1); \tag{35}$$
$$\psi_1(0) = 0, \quad \psi_2(0) = 0. \tag{36}$$

By manipulating Eqs. (32) and (33), the associated modal shapes are given by the following equation:

$$\psi_1(x) = d_1 \cos \omega_w x + d_2 \sin \omega_w x, \tag{37}$$

$$\psi_2(x) = d_3 \cos \omega_w x + d_4 \sin \omega_w x. \tag{38}$$

The nondimensional out-of-plane eigenmodes and natural frequencies can be obtained by

$$\psi(x) = c \sin(m\pi x) \quad \text{and} \quad \omega_w = m\pi \text{ for } m = 1, 2, 3, \ldots \tag{39}$$

where the coefficient c is determined by $\int_0^1 \psi(x)\psi(x)\mathrm{d}x = 1$. In other words, the structure is degenerated into a single cable in the out-of-plane.

4 Effects of the angle at central support

In this study, two independent coordinate systems were chosen to model the two-span suspended transmission lines. However, the behavior of the system reflects the effects of the angle at the central support through the continuity conditions of force and displacement. In order to describe the effect of the parameters on the modal properties comprehensively, the angle of the central support should be taken into account reasonably. For simplicity, we assume that $\theta_1 = \theta_2$. From Table 1, it can be seen that if the two parameters remain the same, what matters is the frequency of the system changing with the parameter θ_1 varying from $\pi/12$ to $\pi/3$. Obviously, for the lower eigenvalues, taking the first frequency as an example, the change is very small (see Table 1). And the results show that with the parameter θ_1 growing, the value increases, while the changing peak differs a little. If one of the parameters $l_1/l_2, b$ remains constant, the frequencies of the system will increase with an increase of the remaining parameters. Beyond that, some other information can be found from the analysis results of the Table 1. For example, after selecting a set of parameters, then contrast the adjacent frequency of the system. It turns out that the angle affects the frequency avoidance phenomena.

5 Concluding remarks

Based on Hamilton's principle, the refined model that describes two-span suspended transmission lines has been presented in this paper. The eigenvalue analysis in the linear in-plane and out-of-plane problems has led to the closed-form solutions of the mode shapes and characteristic frequency equations. The effects of the span ratio and sag-to-span ratio on the natural frequencies of the two-span transmission lines have been investigated as well as those of the inclined angle. It has been shown that these parameters are independent of the first type of eigenvalue solution. Moreover, the characteristic of the mode shape has been examined. It has been shown that the mode shapes are sensitive to the parameter change in the *veering* region, and the mode shapes may exhibit strong localization phenomena. the possible nonlinear interaction of the two-span transmission lines is discussed, such as 1:1 or 1:2 internal resonance.

Similarly, the number of suspended cables is greater than two in the systems of suspended transmission lines. The in-plane and out-of-plane eigenvalue problems are also obtained by referring to the similar inferential

Table 1 Effects of the angle at central support

θ_1	l_1/l_2	b	ω_1	ω_2	ω_3	ω_4	ω_5	ω_6
$\pi/12$	1	0.001	1.2302	2.3649	3.1412	5.7404	6.2832	6.7961
		0.005	1.2392	1.8678	2.4058	3.1172	5.7469	6.2832
	5	0.001	3.1435	6.2832	8.9868	9.4249	12.5664	15.4510
		0.005	3.3751	6.2832	8.9868	9.4340	12.5664	15.4505
$\pi/6$	1	0.001	1.2327	2.3799	3.1411	5.7298	6.2832	6.8051
		0.005	1.2417	1.8583	2.4205	5.7365	6.2832	6.8018
	5	0.001	3.1438	6.2832	8.9869	9.4249	12.5664	15.7080
		0.005	3.4009	6.2832	8.9868	9.4350	12.5664	15.4505
$\pi/3$	1	0.001	1.2425	1.8398	2.4346	3.1385	3.2359	3.6090
		0.005	1.2509	1.8268	2.4715	3.1011	4.5948	4.8438
	5	0.001	3.1453	6.2832	8.9868	9.4249	12.5664	15.4505
		0.005	3.5780	6.2832	8.9868	9.4428	12.5664	15.4505

reasoning method in this paper. Specifically, the boundary and continuity conditions at the central supports between the i-th span and the $(i+1)$-th span are similar to the force conditions and displacement conditions $(i = 1, 2, \ldots)$. Moreover, there is a difference in height between the supports in two-span or multi-span transmission lines; this is a somewhat difficult problem and needs further research.

Acknowledgements The study was supported in the part by the National Natural Science Foundation of China (Grant Nos. 11272119, 11402085), and key Fund Project of Hunan Provincial Department of Education (Grant No. 12A052).

References

1. Paul, C.R.: Analysis of Multiconductor Transmission Lines. Academic Press, Wiley (2008)
2. Irvine, H.: Cable Structures. The MIT Press, Cambridge (1981)
3. Rega, G.: Nonlinear vibrations of suspended cables. Part 1: modeling and analysis. Appl. Mech. Rev. **57**, 443–478 (2004)
4. Perkins, N.C.: Model interaction the non-linear response of elastic cables under parametric/external excitation. Int. J. Non-Linear Mech. **27**, 233–250 (1992)
5. Rega, G.: Theoretical and Experimental Nonlinear Vibrations of Sagged Elastic Cables, vol. 181, pp. 159–210. Springer, Berlin (2012)
6. Srinil, N., Rega, G.: The effects of kinematic condensation on internally resonant forced vibrations of shallow horizontal cables. J. Comput. Nonlinear Dyn. **42**, 180–195 (2007)
7. Wang, L., Zhao, Y.: Nonlinear interactions and chaotic dynamics of suspended cables with three-to-one internal resonances. Int. J. Solids Struct. **43**, 7800–7819 (2006)
8. Lacarbonara, W., Paolone, A., Vestroni, F.: Elastodynamics of nonshallow suspended cables: linear modal properties. J. Vib. Acoust. **129**, 425–433 (2007)
9. Lacarbonara, W.: Nonlinear Structural Mechanics: Theory, Dynamical Phenomena, and Modeling. Springer, New York (2013)
10. Lacarbonara, W., Pacitti, A.: Nonlinear modeling of cables with flexural stiffness. Math. Probl. Eng. (2008), Article ID 370767, p. 21
11. Arena, A., Pacitti, A., Lacarbonara, W.: Nonlinear response of elastic cables with flexural-Torsional stiffness. Int. J. Solids Struct. **87**, 267–277 (2016)
12. Claren, R., Diana, G.: Mathematical analysis of transmission line vibration. Inst. Electr. Electron. Eng. Trans. Power Appar. Syst. **60**, 1741–1771 (1969)
13. Kraus, M., Hagedorn, P.: Aeolian vibration: wind energy input evaluated from measurements on an energized transmission lines. Inst. Electr. Electron. Eng. Trans. Power Deliv. **6**, 1264–1270 (1991)
14. Verma, H., Hagerdorn, P.: Wind induced vibration of long electrical overhead transmission line spans: a modified approach. J. Wind Struct. **8**, 89–106 (2004)
15. Chan, J.K., Lu, M.L.: An efficient algorithm for Aeolian vibration of single conductor with multiple dampers. Inst. Electr. Electron. Eng. Trans. Power Deliv. **22**, 1822–1829 (2007)
16. Barry, O., Zu, J.W., Oguamanam, D.: Analytical and experimental investigation of overhead transmission lines vibration. J. Vib. Control **21**, 2825–2837 (2015)
17. Barry, O., Zu, J.W., Oguamanam, D.: Forced vibration of overhead transmission line: analytical and experimental investigation. J. Vib. Acoust. **136**, 041012 (2014)
18. Liang, S.G., Ma, Z.X.: An analysis of wind-induced response for Dashengguan electrical transmission tower-line system across the Yangtze River. In: Proceedings of the 10th International Conference on Wind Engineering, pp. 565–570 (1999)
19. Clough, R.W., Penzien, J.: Dynamic of Structures, 3rd edn. McGraw-Hill, New York (2003)
20. Gattulli, V., Lepidi, M.: Localization and veering in the dynamics of cable-stayed bridges. Comput. Struct. **85**, 1661–1678 (2007)
21. Natsiavas, S.: Mode localization and frequency veering in a non-conservative mechanical system with dissimilar components. J. Sound Vib. **165**, 137–147 (1993)